INTER FIBRE CRACKING BEHAVIOUR OF CFRP UNDER VERY HIGH CYCLE FATIGUE LOADING: EXPERIMENTAL AND ANALYTICAL MULTI-SCALE APPROACH

Gordon Just, Ilja Koch, Mike Thieme and Maik Gude

Institute of Lightweight Engineering and Polymer Technology, Technische Universität Dresden
Holbeinstraße 3, 01307 Dresden, Germany
Email: gordon.just@tu-dresden.de , web page: http://www.tu-dresden.de/mw/ilk

Keywords: CFRP, energy release rate, fracture, VHCF

ABSTRACT

For the analysis of the critical inter fibre cracking behaviour of cross-ply carbon fibre reinforced plastics (CFRP) at very high cycle fatigue (VHCF) loading, specific test principals and a shaker based bending fatigue test stand have been developed. With the help of the presented test stand the experimental characterisation of inter fibre cracking of CFRP under fully reversed fatigue is performed. Multiple cracking events on the specimen surface were recorded by light microscopy and statistically analysed. The homogeneous stress/strain distribution at the specimen surface facilitates the determination of SN curves as each occurring crack is considered to be one failed separated specimen.

It is therefore convenient to analyse the local stress/strain distributions between adjacent cracks by finite fracture mechanics. Two different models are used to describe the tensile and bending fatigue experiments, respectively. Furthermore, a comprehensive fatigue model based on the calculation of the mechanical energy release rate in the off-axis plies is derived, which is capable of describing and predicting the inter fibre failure observed in the bending experiments. Based on the evaluation of the bending fatigue tests, the model also predicts the cracking events of the tensile fatigue tests in a suitable way. The first experimental results and modelling approaches are presented and discussed in this paper proving the suitability of the chosen models to describe the fatigue behaviour and material degradation throughout the experiment.

1 INTRODUCTION

The rapidly developing market of continuous carbon fibre reinforced polymers in wind energy, aerospace and automotive engineering among others demands for reliable testing and damage evaluation methods. Due to the multi-axial loads occurring during service life, inter fibre failure may develop in off-axis plies either due to the off-axis loading or due to interaction with neighbouring plies. Those cracks are known to influence the mechanical properties of the structure, as well as they represent pathways through which corrosive agents may penetrate into the laminate. Another major concern is that the transverse cracks may act as nuclei for delaminations or longitudinal splitting in the laminates causing premature failure [1-6].

The damage and fatigue behaviour of FRP has been extensively studied within the high cycle fatigue (HCF) regime. Mainly due to inacceptable long test durations and thus expensive testing, only few experiments were performed above 10^7 loading cycles [7]. Considering wind or aircraft turbines, the required service life of technical applications often exceeds the range of high cycle fatigue and it is known that inter fibre failure (IFF) may occur beyond this point. Therefore it becomes necessary to shorten the test duration to achieve reliable testing results within reasonable time.

Furthermore, it is essential to describe and predict the fatigue behaviour within the VHCF regime with the help of suitable models, which account for micro cracking in the off-axis plies, considering crack growth and stress redistribution.

2 EXPERIMENTAL SETUP AND MATERIALS

2.1 Test stand

In order to perform time and cost efficient fatigue experiments, it is favourable to test the specimens at sufficiently high testing frequencies without significant specimen heating, which can lead to premature failure. Therefore, the bending fatigue experiments are performed using an improved version of the recently developed shaker based VHCF test stand [8], as shown in Fig. 1. The specimen is loaded by the acceleration force of eccentric masses, which are oscillating due to shaker excitation. The axes of rotation of the eccentric masses do not coincide with the specimen clamping by purpose. Therefore the clamping is axially guided aiming at minimized axial forces in the specimen. Hence, the specimen is loaded in pure bending resulting in a homogeneously stressed specimen surface. Due to the absence of shear forces the specimen does not exhibit significant heating. To prevent additional heat flux from the shaker table into the test stand a water-cooled base plate is attached underneath the test stand (not shown in Fig. 1). It should be noted that the bending fatigue experiment has several advantages compared to conventional tension experiments, e.g. the small volume that is stressed during the test and the lower forces necessary to apply the required deformation.

By the use of two *WayCon*© LAM-10 laser sensors the position of the midpoint of the specimen and test stand position are measured and used to determine the specimen deflection. In conjunction with measuring the rotation of the specimen clamping by magnetic angle sensors, the maximum specimen surface strain can be calculated on-line. The specimen behaviour can now be monitored in short time intervals and the experiment stops automatically in case of a significant increase of specimen amplitude, which is an indicator for the development of inter fibre cracks.

For comparison, tension-tension fatigue experiments on conventional servo-hydraulic testing machines were conducted at Technical University Hamburg-Harburg (TUHH).

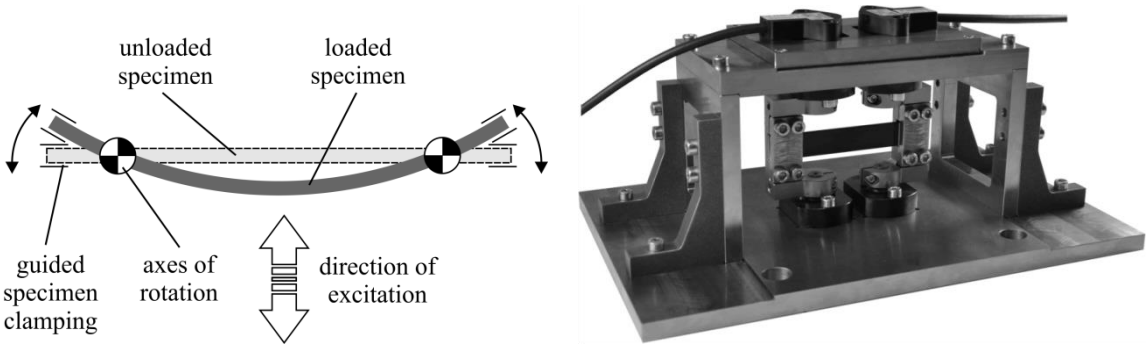

Figure 1: (a) Operating principle of the bending test stand and (b) test stand with clamped specimen

2.2 Specimen design and materials

The CFRP used within the experiments consist of a T700SC (*Toray*) fibre reinforcement with epoxy resin compatible sizing arranged as non-twisted 12 k roving. The resin in use is the Huntsman Araldite LY 1556/Aradur1571/Accelerator 1573/Hardener XB 3403. The composite laminates were made by prepregs, which were specifically fabricated at TUHH by use of an in-house impregnation machine. Here a 300 mm wide, unidirectional tape with straight, aligned fibres is produced. The final composite plates are cured in a heat press at 120 °C [8, 9]. The resulting ply properties are listed in Tab. 1.

Due to the different testing setups (tension and bending) diverse specimens with varying dimensions and lay-ups were produced. The tension-tension specimens were manufactured in accordance to DIN EN ISO 527-4 with a specimen thickness of 2 mm and end tabs to facilitate specimen clamping. A symmetrical $[0/90_n]_s$ cross-ply lay-up was used for the static and fatigue tests resulting in a 0°-ply thickness of about 0.3 mm. The tension fatigue loading was applied at a test frequency of 6 Hz and a stress ratio of R = 0.1. For examination of the fatigue life, three load levels were tested: 745 MPa, 651 MPa and 605 MPa maximum stress, which correspond to 80 %, 70 % and

65 % of the mean tensile strength of the laminate, respectively. The experiments were conducted within the HCF regime up to 10^6 cycles and stopped at specific number of cycles to investigate the cracking state of the specimens.

Since testing at a frequency of 6 Hz would lead to unacceptable long testing durations within the VHCF regime (testing 10^7 load cycles would require more than 19 days), the tests were conducted with the bending fatigue test stand at elevated testing frequencies. In the bending fatigue tests a symmetrical $[90/0_n]_s$ lay-up was used in order to apply the 90°-layer in the area of maximum strain. The specimens with the dimensions 100 mm × 15 mm (length × width) were cut out of the laminate plates with a high precision abrasive cutting machine. As the specimen is part of the vibrating system, its stiffness has an impact on the eigenfrequency of the whole testing system.

Longitudinal Young's modulus [GPa]	Transverse Young's modulus [GPa]	In-plane shear modulus [GPa]	Out-of-plane shear modulus [GPa]	In-plane Poisson's ratio (ν_{12}) [–]	Out-of-plane Poisson's ratio [–]
127.4	8.68 ± 0.48	2.5*	3.1*	0.28	0.418
Transverse tensile strength [MPa]	Transverse strain to failure [MPa]				
61 ± 2	0.74 ± 0.04				

* Approximated values

Table 1: Mechanical properties of the unidirectional ply (fibre: T700SC, resin: Araldite LY 1556/Aradur1571/Accelerator 1573/Hardener XB 3403)

Specimens with a thickness of 2 mm and 3 mm were manufactured with a constant 90°-ply thickness of 0.3 mm and 0°-supporting layer thicknesses of 1.4 mm and 2.4 mm, respectively. As the specimen stiffness is mainly influenced by the thickness of the supporting layer the achieved testing frequencies for the 2 mm and 3 mm thick specimens range from 60 Hz up to 150 Hz, respectively. The fully reversed (R = -1) bending fatigue tests were performed at strain levels between 0.002 to 0.00475 maximum flexural strain. In order to investigate crack propagation through the transverse ply thickness, the samples were polished along the free edges.

3 EXPERIMENTAL RESULTS

3.1 Cracking behaviour

As described in section 2.1, it is possible to detect an increase of the specimen deflection during testing and to automatically stop the bending experiment in case of exceeding the pre-defined threshold. The specimen is then demounted from the test stand and examined by intermittent light microscopy. Considering Fig. 2 (a), the cracks can be clearly identified at the specimen surface. The crack tips are focussed and their positions are examined by a cross table with tracking capability. Consequently, the cracks can be recovered in subsequent examinations and crack extension can be tracked. The cracks appear to generally spread about the whole specimen width instantly, covering the total cross section of the 90°-ply. Due to the brittle nature of the material, stable crack propagation with cracks not spanning the entire specimen width is rarely determined. The position, length and number of cracks are taken into account for statistical means and the modelling approach presented in section 4.

As already recorded by other authors [10-12] the inter fibre failure (IFF) is dominated by interfacial failure with subsequent crack propagation connecting the failed interfaces, as shown in Fig. 2 (b). However, the through-thickness crack propagation takes place very fast and could not be observed in situ by the authors.

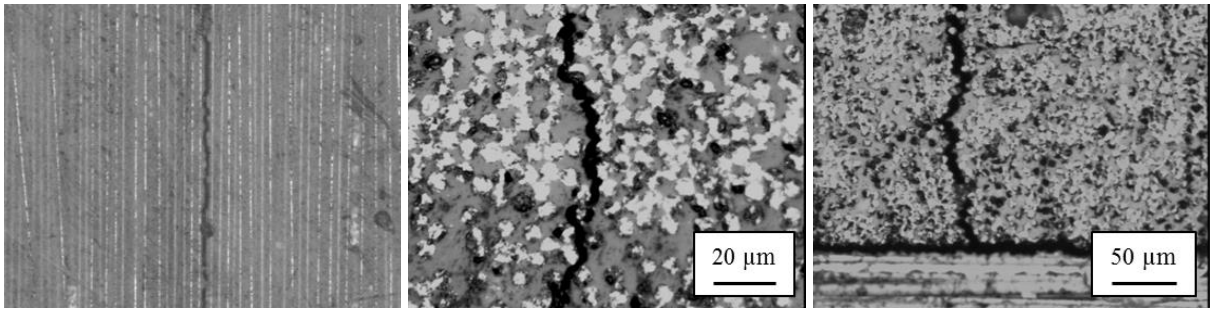

(a) top view (specimen surface) (b) side view (polished edge) (c) side view (polished edge)

Figure 2: (a) Inter fibre failure at the specimen surface, (b) interface dominated IFF and (c) crack branching into delamination at the ply interface

During the course of testing, the initiation and growth of delaminations beginning at the crack tips of the 90°-plies was also observed, as depicted in Fig. 2 (c). Contrary to the transverse cracks, the quantification of the delamination geometry and size is very difficult, since the delaminations cannot be seen completely from the specimen side. Nevertheless, the characterisation of the delamination area is a task currently pursued by computer-tomography.

Regarding the tension-tension specimens, the cracking behaviour is characterised by X-ray examinations, since the 90°-ply is bounded by the 0°-plies and the cracks can only be observed at the specimen edges by means of light microscopy. After reaching a specific number of cycles, the samples were demounted from the testing machine and treated with a contrast agent based on zinc iodide (ZnI_2). The cracks were found to be located arbitrary along the specimen length, but are mostly evenly spaced. The majority of the cracks spreads along the whole specimen width, but some cracks were covering only parts of the total width. It is still unclear, whether these cracks are not fully developed or the contrast agent could not penetrate into the whole crack length. Further investigations will be performed to clarify the crack growth in the specimen width direction.

3.2 Damage kinetics

The observed cracking behaviour does not show a gradually increase of cracks or crack length. Instead, multiple cracking at arbitrary positions along the free specimen surface is recognized for both tests. It is therefore convenient considering the crack density of the 90°-test layers. In the following, the crack density $D = i/l$ is defined as the number of cracks i along the evaluation path l = 65 mm for bending and l =50 mm in case of tension-tension experiments.

Considering the tension-tension experiments, at high loading a large number of cracks developed within the first fifty cycles, resulting in crack densities between 0.34 and 0.44 1/mm. In the further course of the fatigue experiments an increase in crack density with subsequent saturation at high levels of crack density was determined as shown in Fig. 3. At this point the cracks are spread all over the examined specimens with an almost even crack spacing. This distinct formation of inter fibre cracks is observed before final failure of the laminate and has been termed as characteristic damage state (CDS) by Reifsnider and Talug [13].

In contrast, the load levels applied within the bending fatigue experiments are chosen rather low for investigating the crack development in the VHCF regime. The formation of cracks at VHCF relevant load levels (ε = 0.3 … 0.4 %) was found to show a delayed behaviour. Although the loading was kept very low, cracks formed beyond 10^6 cycles. In conjunction with the homogeneously stressed specimen surface, only few cracks form arbitrary along the testing length and are not found to be spaced uniformly. Additionally, the number of cracks forming during the tests is quite low in comparison to the tension-tension fatigue experiments.

The cracking state of the specimens, as seen in Fig. 3, is used to describe the fatigue behaviour of the cross-ply laminates, based on energy methods and analytical models. Recalling that the tested specimens consist of the same material but the test procedures are different, the results cannot be compared directly. Therefore, the following approach based on energy methods and analytical solutions is proposed.

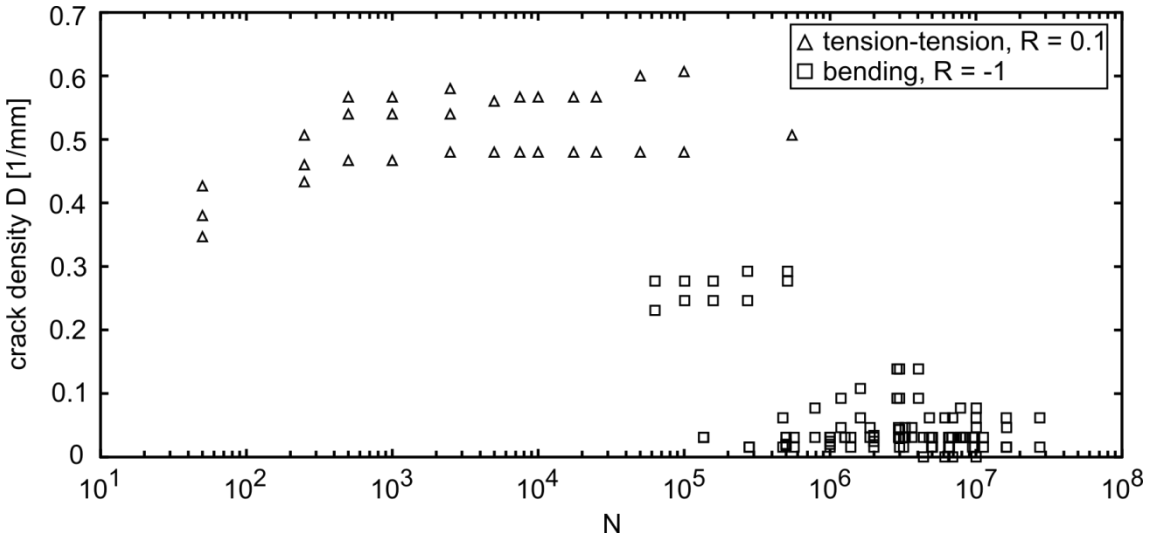

Figure 3: Crack densities recorded for tension-tension and bending fatigue specimens at different strain levels

4 ENERGY BASED MODELLING APPROACH

Although the procedure of testing differs between the tension-tension and bending experiments, the damage phenomena are comparable. As mentioned before, the specimen behaviour is governed by inter fibre failure in both cases, but the transverse plies are constrained differently. In case of the tension-tension experiments the transverse ply is constrained on top and bottom symmetrically by the adjacent 0°-plies. In bending the outer 90°-plies are unconstrained at the free specimen surface and only constrained on one side by the 0°-ply.

Hashin [14] and Vinogradov and Hashin [15] proposed an analytical solution to calculate the residual stiffness and energy release rate (ERR) due to crack formation for cross-ply laminates using variational analysis. The model is based on describing the stress distribution between two adjacent cracks by introducing stress perturbation functions $\phi_i(x)$ to the ply stresses in each ply assuming the ply stresses to be functions of x (loading direction) only and constant throughout the ply thickness. The geometric conditions in the model are equal to those in the tension-tension experiment and depicted in Fig. 4.

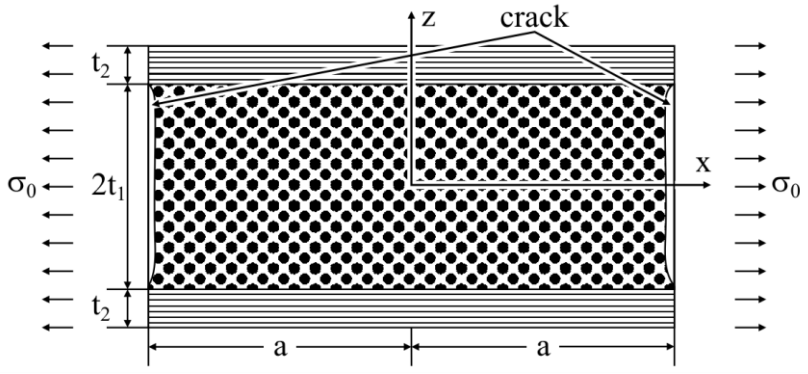

Figure 4: Laminate region between two adjacent cracks (following [14])

The perturbation stresses are calculated by considering the equilibrium equations for the plies

$$\frac{\partial \sigma_{xx}^{m}}{\partial x} + \frac{\partial \sigma_{xz}^{m}}{\partial z} = 0, \tag{1}$$

$$\frac{\partial \sigma_{xz}^{m}}{\partial x} + \frac{\partial \sigma_{zz}^{m}}{\partial z} = 0, \tag{2}$$

where σ_{ij} ($i,j = x,y,z$) denotes the perturbation stresses in the plies and m is the ply index. Using the appropriate boundary conditions, as discussed in [14], an admissible stress field is derived. Following Hashin and minimizing the complementary energy as well as solving the differential equation for ϕ, the change of complementary energy between two cracks due to crack formation U' can be expressed in the simple form

$$U' = \sigma_{1t}^2 t_1^2 C_{2t} \chi(\rho), \tag{3}$$

where σ_{1t} is the ply stress in the transverse ply, t_1 is half the thickness of the transverse ply, C_{2t} is a constant depending on the material and laminate properties and $\chi(\rho)$ is a form function depending on the crack spacing $\rho = a/t_1$. According to Vinogradov and Hashin [15] the mechanical energy release rate G_t due to formation of a new crack midway between two existing cracks (uniform crack spacing) in the inner transverse ply when loaded in tension can then be written as

$$G_t = \sigma_{1t}^2 t_1 C_{2t} \left(2\chi\left(\frac{\rho}{2}\right) - \chi(\rho)\right). \tag{4}$$

In analogy to that, Kim and Nairn [16] presented an analytical model to describe multiple cracking in coating/substrate systems especially for bending loads. For developing the approach a bending moment is applied resulting in pure bending which is similar to the loading situation induced by the VHCF test stand described in section 2. The coating layer is considered to be on the outer specimen surface loaded in tension and the cracks are supposed to form in a uniform pattern by multiple cracking as it is commonly observed for coatings. The coating/substrate system is very similar to the $[90/0_n]_s$ cross-ply laminate used in bending fatigue with its stiff supporting layer (substrate) and the brittle off-axis testing layer (coating).

Based on the solution of a similar differential equation, as introduced by Hashin [14] before, but accounting for the change in ply constrains and an adopted calculation of the ply stress for the bending case, the mechanical energy release rate depending on the crack density D can be expressed as

$$G_b = \sigma_{1b}^2 t_1 C_{2b} 2Y(D), \tag{5}$$

$$Y(D) = \left[2\chi\left(\frac{\rho}{2}\right) - \chi(\rho)\right], \tag{6}$$

where C_{2b} is a constant calculated with respect to the bending case, the crack spacing $\rho = 1/(2t_1 D)$ and the effective bending stress σ_{1b}, which is calculated in terms of

$$\sigma_{1b} = -\frac{2z_1}{B} E_c \varepsilon_b, \tag{7}$$

with the (transverse) Young's modulus of the coating layer E_c, the effective bending strain ε_b, the half specimen thickness B and z_1 as the position of the midpoint of the coating layer relative to the neutral axis. These analytical solutions are used afterwards to calculate the energy release rate for the formation of a complete crack in the transverse ply.

In this paper Hashin's solution (equation (4)) is used for modelling the conventional tension-tension fatigue experiments with inner 90°-layers and the model proposed by Nairn and co-workers (equation (5)) is utilized for modelling the bending fatigue experiments with outer 90°-layers. For simplicity, residual stresses have been ignored in the following calculations, but will be considered in future work. However, as the residual stresses influence the results for static loads as well as for fatigue loading, the effect on the results presented hereafter is considered to be rather small.

4.1 Model verification and determination of ERR under static loading

To verify the presented analytical solution for the specimens, three samples were tested in quasistatic four-point bending. The samples were conditioned in standard atmosphere and tested in accordance to DIN EN ISO 14125. The specimens were loaded up to a specific surface strain and unloaded subsequently. With the aid of microscopic investigations the number of cracks at the specimen surface loaded in tension was determined after each loading cycle. Therefore only the mid-area of the specimens between the two dies was considered, because of the pure bending load within

this area. The recorded crack densities D_{exp} for all experiments at the applied bending strain levels ε_b are shown in Fig. 5 (circles).

Assuming that the next crack forms when the mechanical energy release rate exceeds a critical, material dependent value $G_{b,stat}$, the experimental result can well be modelled by solving equations (5) and (7) for the applied strain. For bending loads, the solution is

$$\varepsilon_b = -\frac{B}{2z_1 E_c}\sqrt{\frac{G_{b,stat}}{t_1 C_{2b} 2Y(D)}}\,. \tag{8}$$

Since the crack density D is implicitly given by $Y(D)$, the solution of equation (8) can be directly plotted as a function of the crack density instead of $Y(D)$ itself. Fitting the analytical solution to the experimental data yields an energy release rate of $G_{b,stat}$ = 400 J/m² in case of static loading. For crack densities ranging from D = 0 to D = 1, the predicted bending strain is determined as the solid line in Fig. 5. The energy release rate $G_{b,stat}$ is interpreted as a material constant for the formation of one transverse crack through the entire cross section of the 90°-plies and is assumed to be identical for the tension-tension specimens. It is named G_{stat} in the further course of this paper. Nevertheless, G_{stat} is not strictly identical to the energy release rate G_{Ic}, which characterizes the crack growth in the sense of linear elastic fracture mechanics (LEFM). G_{stat} describes the formation of one complete crack through the entire cross section of a transverse ply and is used to describe multiple cracking in off-axis layers. As these cracks have a distinct size the theory of multiple cracking has been named finite fracture mechanics by Vinogradov and Hashin [15].

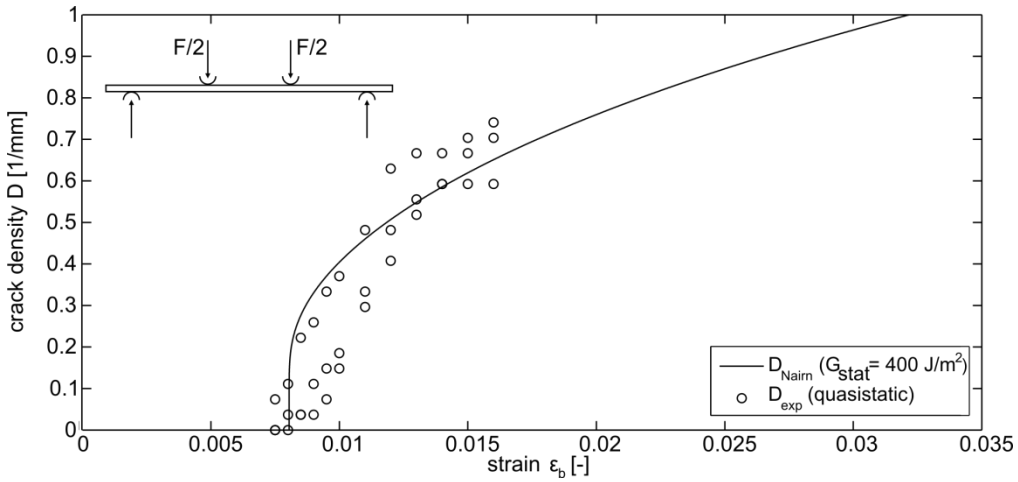

Figure 5: Crack densities recorded in quasistatic bending experiments (circles) and analytical solution for outer ply cracks (solid line, $G_{b,stat}$ = 400 J/m²)

In the static bending experiment no cracks could be observed throughout the whole experiment on the specimen surface loaded in compression, leading to the assumption that the critical energy release rate was not exceeded. This could be explained by the mode of failure that differs from the one in case of tension loading. The cracks in the transverse plies loaded in tension are considered to be mode I cracks, whereas in case of compression loading the cracks are usually governed by shear stresses, leading to mode II crack propagation.

4.2 Application to cyclic loading

Applying these models to the fatigue experiments in tension-tension and bending requires the calculation of the energy release rates during the fatigue loading. As the loading is applied periodically the range of G_b, denoted as ΔG_b, is used instead of G_b. Using the relation between the maximum and minimum stress values $\sigma_{min} = R\sigma_{max}$, the range of the energy release rate for values of $R \geq 0$ can be written as

$$\Delta G = (1 - R^2) G_{max}\,. \tag{9}$$

The experimental maximum energy release rates for the tested load levels were calculated with respect to the real cracking state of the samples as recorded during the fatigue tests. Using equations (4) and (5) with equation (9) for tension-tension and bending fatigue respectively, the range of the energy release rate ΔG is calculated with respect to the crack density and the applied load. Considering the bending experiment and reminding that no cracks due to compression loading have been observed within the quasistatic tests, the amplitude of the ERR, G_{max}, is used as ΔG. As exemplarily shown for one load level in Fig. 6 (a), the mechanical energy release rate is slightly higher for the tension experiment compared to bending case at a comparable strain level.

The differences are caused by the specimen lay-up. In case of the tension specimen, the transverse ply is thicker with $t_{1,t} \approx 0.7$ mm than the 90°-ply in bending with $t_{1,b} \approx 0.3$ mm. At the same strain level the mechanical energy release is higher and the specimen is developing cracks faster for thicker plies than the sample with thinner plies. This is in agreement with Kim and Nairn [16], who stated that thicker coatings tend to crack sooner than thin coatings when loaded equally. Furthermore, the transverse plies are constrained differently by the 0°-plies. The development of cracks leads to crack shielding effects, influencing the stress transfer from the load carrying 0°-plies into the 90°-ply. As a result, the stresses between two adjacent cracks may diminish more significantly in case of highly constrained inner transverse plies than in the less constrained case of outer transverse plies, leading to a significant decrease of the mechanical energy release for high crack densities (see Fig. 6 (a)).

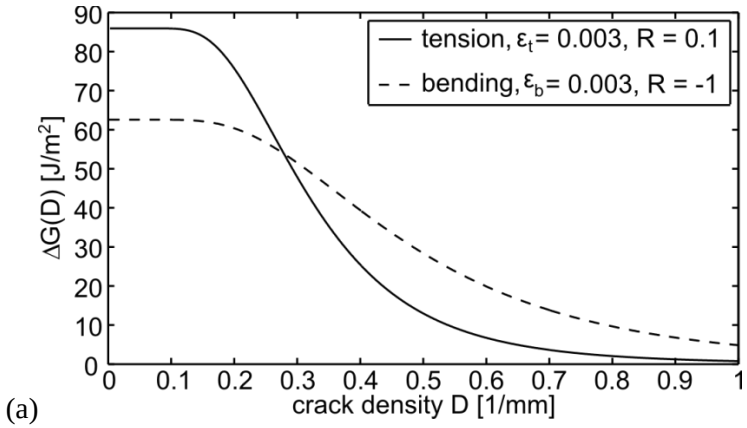

(a)

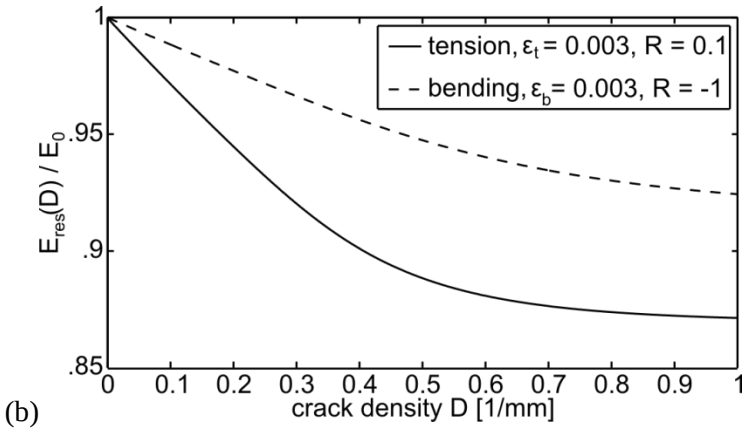

(b)

Figure 6: (a) Calculated range of the energy release rate G_{max} in case of bending ($[90/0_n]_s$) and tension ($[0/90_n]_s$) for tested specimens and (b) predicted stiffness reduction due to crack formation for 2 mm thick specimens at comparable load levels

As a second result of the described models, the residual laminate stiffness due to crack formation $E_{res}(D)$ can be calculated for the tension-tension and bending specimens, which is commonly used to describe the laminate condition in fatigue testing [6]. As shown in Fig. 6 (b), the decrease in laminate stiffness is significantly higher in case of tensile loading. This is mainly attributed to the thick 90°-ply

in the tensile specimen, which severely affects the residual stiffness of the specimen in case of crack development. The influence is less significant in case of the thin off-axis plies used for the specimens in bending fatigue. For sufficiently high crack densities, the residual stiffness reaches an asymptotic value, denoting a fully cracked off-axis ply with stiffness reduced to zero.

The experimentally determined crack densities recorded after a certain number of cycles are used in conjunction with the range of mechanical energy release (Fig. 6 (a)) resulting in an expression of the crack densities *D(N)* as a function of number of cycles. In consequence the range of mechanical energy release can be interpreted in terms of number of cycles and therefore be used to describe the fatigue behaviour of the specimens.

4.3 Comprehensive description of fatigue experiments

As stated before the experiments are not directly comparable, since they differ in the method of testing, specimen geometry, lay-up and stress ratio. By the use of energy methods a promising approach for comprehensively describing the inter fibre failure of both experiments and enabling the comparison of these two different experiments has been found.

Since the deflection amplitudes are rather low in the fatigue experiments, linear elastic material behaviour is assumed. It can be shown, that the normalized range of the mechanical energy release rate ΔG by the quasistatic value G_{stat} is equal to the range of the square of the stress based material effort $\Delta(F^2)$ according to

$$\frac{\Delta G}{G_{stat}} = \Delta(F^2)\ . \tag{10}$$

It is given similarly to the equivalent strain energy approach, which defines the material effort as a failure mode specific equivalent stress divided by the material strength [17]. According to equation (10), the equivalent energy release rate has now been calculated for all cracking events recorded in the tensile and bending experiments. As proposed by Koch [17] the best fit for the experimental data points is obtained by use of a wear-out model expressed by the equation

$$\Delta(F^2) = \left(\frac{1-V_w}{N-V_w}\right)^{N_w}\ , \tag{11}$$

where N is the number of cycles for each cracking event and V_w and N_w are coefficients determined by fitting to the experimental data. The experimental data for both experimental setups and the prediction of the fatigue behaviour by equation (11) based on the bending fatigue experiments only are shown in Fig. 7.

Regarding the results for the tension-tension fatigue experiments it can clearly be seen, that they can be predicted well by the presented approach. However, some data points recorded within the tensile experiments do not fit very well (Fig. 7, shaded triangles). This is mainly caused by misleaded processing of experimental data from high load levels. From an experimentally point of view, the moment of crack observation does not coincide directly with the moment of the actual cracking event, as the tests were stopped at distinct time points, no matter whether cracks have already occurred earlier or not. In consequence, the number of cycles used to plot the results does not match with the exact moment of crack initiation and is therefore shifted to a higher number of cycles. Additionally, the range of the energy release rate is calculated based on the maximum stress applied. Since the tensile specimens are experiencing high loading, some cracks may initiate already before the maximum stress in the transverse ply is reached in the initial loading step. Thus, the calculated range of the energy release rate is overpredicted when the maximum stress is used for calculation. Using the exact stresses at crack initiation leads to a shift of the data points to lower, more reasonable values of ΔG. However, since the experiments were first stopped after fifty load cycles, the exact stresses at crack initiation in the initial loading step were not determined.

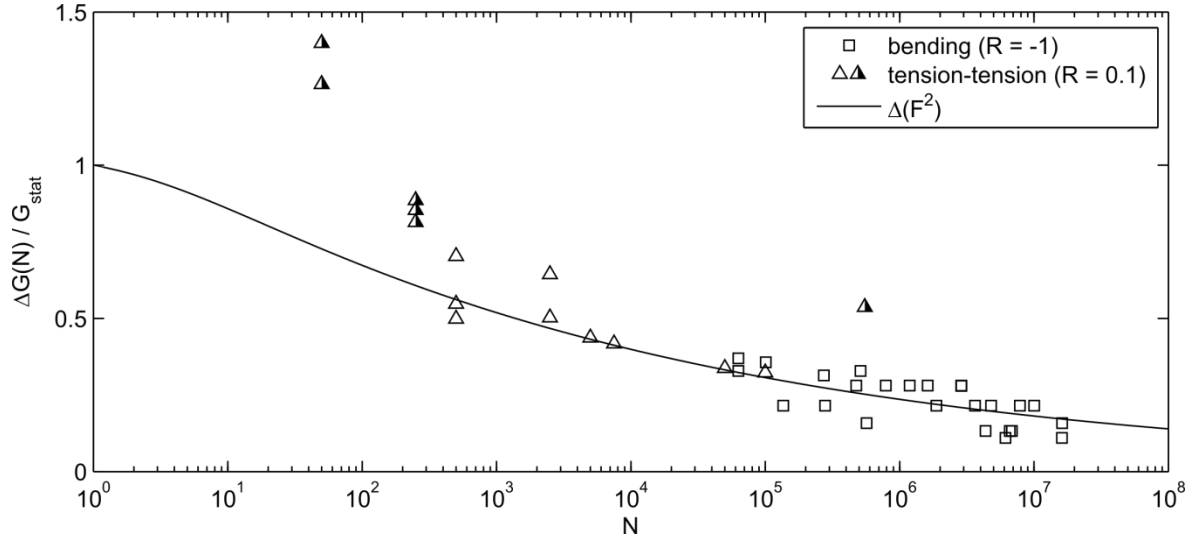

Figure 7: Normalized range of the mechanical energy release rate in case of newly observed cracks for tension-tension (triangles) and bending fatigue experiments (rectangles) and prediction of the fatigue behaviour by equation (11)

Considering data points for $N > 3\times10^2$ cycles the model is suitable to describe and predict the initiation of transverse cracks in a unified way for different loading types, stress ratios, lay-ups and off-axis layer thicknesses.

In order to determine a technical crack initiation fatigue limit for 10^8 loading cycles, the extrapolation of the prediction model is used. As a result, allowable stress and strain amplitudes in the transverse plies for the bending experiments are calculated to $\sigma_a \leq 21.88$ MPa and $\varepsilon_b \leq 0.0025$ respectively. Currently ongoing experiments with strain amplitudes of $\varepsilon_b < 0.0025$ bending strain are promising to verify these results.

5 CONCLUSION

In this paper, an energy based modelling approach to describe and predict the inter fibre cracking behaviour under HCF and VHCF loading for cross-ply laminates has been presented. The findings are based on a shaker based bending fatigue test stand, which has been developed and successfully used for very high cycle fatigue testing. Additional conventional tension-tension fatigue tests are used for validation.

The mechanical energy release rate necessary to form one complete crack in the transverse ply was calculated for the fatigue experiments, accounting for the actual cracking state and fatigue loading using finite fracture mechanics models proposed by Hashin and Kim and Nairn. By normalization with the mechanical energy release rate obtained in quasistatic testing it is possible to predict the fatigue behaviour in terms of a wear-out model. It was shown, that the approach is suitable to describe different sets of experiments, which differ in the way of testing, the specimen design, load ratio and the load level. It is furthermore possible to determine allowable stress or strain amplitudes for a technical fatigue limit of 10^8 load cycles without the necessity of testing for the whole lifetime.

The verification of the modelling approach is still in progress, but current tests are promising. The presented approach will be further investigated for other load ratios and materials to improve its accuracy and reliability.

ACKNOWLEDGEMENTS

The authors gratefully thank the German Research Foundation (DFG) for their financial support within the priority program SPP 1466 and the project partner at Technical University Hamburg-Harburg (TUHH), namely Prof. Fiedler et al., for supplying the testing material and experimental data in tension-tension fatigue.

REFERENCES

[1] S. Adden, P. Horst, Stiffness degradation under fatigue in multiaxially loaded non-crimped-fabrics, *International Journal of Fatigue*, **32**, 2010, pp. 108-122 (doi:10.1016/j.ijfatigue.2009.02.002)

[2] F. Ellyin, M. Martens, Biaxial fatigue behaviour of unidirectional filament-wound glass-fiber/epoxy pipe, *Composite Science and Technology*, **61**, 2001, pp. 491-502, (doi:10.1016/S0266-3538(00)00215-3)

[3] P. Mertiny, A. Gold, Quantification of the leakage damage in high-pressure fibre-reinforced polymer composite tubular vessels, *Polymer Testing*, **26**, 2007, pp. 172-179, (doi:10.1016/j.polymertesting.2006.09.009)

[4] S. Ogihara, N. Takeda, Interaction between transverse cracks and delamination during damage progress in CFRP cross-ply laminates, *Composites Science and Technology*, **54**, 1995, pp. 395-404, (doi:10.1016/0266-3538(95)00084-4)

[5] S. Ogihara, N. Takeda, S. Kobayashi, A. Kobayashi, Effects of stacking sequence on microscopic fatigue damage development in quasi-isotropic CFRP laminates with interlaminar-toughened layers, *Composites Science and Technology*, **59**, 1999, pp. 1387-1398, (doi:10.1016/S0266-3538(98)00180-8)

[6] M. Gude, W. Hufenbach, I. Koch, Damage evolution of novel 3D textile-reinforced composites under fatigue loading conditions, *Composites Science and Technology*, **70**, 2010, pp. 186-192, (doi:10.1016/j.compscitech.2009.10.010)

[7] A. Hosoi, N. Sato, Y. Kusumoto, K. Fujiware, H. Kawada, High-cycle fatiguecharacteristics of quasi-isotropic CFRP laminates over 10^8 cycles (Initiation and propagation of delamination considering interaction with transverse cracks), *International Journal of Fatigue*, **32**, 2010, pp. 29-36, (doi:10.1016/j.ijfatigue.2009.02.028)

[8] M. Gude, W. Hufenbach, I. Koch, R. Koschichow, K. Schulte, J. Knoll, Fatigue testing of carbon fibre reinforced polymers under VHCF loading, *Procedia Materials Science*, **2**, 2013, pp. 18-24, (doi: 10.1016/j.mspro.2013.02.003)

[9] J.B. Knoll, B.T. Riecken, N. Kosmann, S. Chandrasekaran, K. Schulte, B. Fiedler, The effect of carbon nanoparticles on the fatigue performance of carbon fibre reinforced epoxy, *Composites: Part A*, **67**, 2014, pp. 233-240, (doi:10.1016/j.compositesa.2014.08.022)

[10] E.K. Gamstedt, B.A. Sjögren, Micromechnisms in tension-compression fatigue of composite laminates containing transverse plies, *Composites Science and Technology*, **59**, pp. 167-178, (doi:10.1016/S0266-3538(98)00061-X)

[11] T.J. Vaughan, C.T. McCarthy, A micromechanical study on the effect of intra-ply properties on transverse shear fracture in fibre reinforced composites, *Composites: Part A*, **42**, 2011, pp. 1217-1228, (doi:10.1016/j.compositesa.2011.05.004)

[12] E. Correa, V. Mantič, F. París, A micromechanical view of the inter-fibre failure of composite materials under compression transverse to the fibres, *Composites Science and Technology*, **68**, 2008, pp. 2010-2021, (doi:10.1016/j.compscitech.2008.02.022)

[13] K.L. Reifsnider, A. Talug, Analysis of fatigue damage in composite laminates, *International Journal of Fatigue*, **2**, 1980, pp. 3-11, (doi:10.1016/0142-1123(80)90022-5)

[14] Z. Hashin, Analysis of cracked laminates: a variational approach, *Mechanics of Materials*, **4**, 1985, pp. 121-136, (doi:10.1016/0167-6636(85)90011-0)

[15] V. Vinogradov, Z. Hashin, Probabilistic energy based model for prediction of transverse cracking in cross-ply laminates, *International Journal of Solids and Structures*, **42**, 2005, pp. 365-392, (doi:10.1016/j.ijsolstr.2004.06.043)

[16] S.-R. Kim, J.A. Nairn, Fracture mechanics analysis of coating/substrate systems Part I: Analysis of tensile and bending experiments, *Engineering Fracture Mechanics*, **65**, 2000, pp. 573-593, (doi:10.1016/S0013-7944(99)00141-1)

[17] I. Koch, Modellierung des Ermüdungsverhaltens textilverstärkter Kunststoffe, *PhD thesis*, TU Dresden, 2010